An Atypical Human Induced Pluripotent Stem Cell Line With a Complex, Stable, and Balanced Genomic Rearrangement Including a Large De Novo 1q Uniparental Disomy

CLARA STEICHEN,[a,b,c] JÉRÔME MALUENDA,[d,*] LUCIE TOSCA,[e,*] ELÉANOR LUCE,[a,b,c] DOMINIQUE PINEAU,[e]
NOUSHIN DIANAT,[a,b,c] ZARA HANNOUN,[a,b,c] GÉRARD TACHDJIAN,[e] JUDITH MELKI,[d]
ANNE DUBART-KUPPERSCHMITT[a,b,c]

Key Words. Induced pluripotent stem cells • Genomic integrity • Uniparental disomy •
Abnormal karyotype • Teratoma formation • Directed differentiation

[a]INSERM U972 and
[c]Département Hospitalo-
universitaire Hepatinov, Paul
Brousse Hospital, Villejuif,
France; [b]Unité Mixte de
Recherche (UMR) S972,
Université Paris-Sud, Paul
Brousse Hospital, Villejuif,
France; [d]INSERM UMR S986,
Institut Fédératif de
Recherche 93, Bicêtre
Hospital, Kremlin-Bicêtre,
France; [e]Department of
Cytogenetics, Béclère
Hospital, Clamart, France

*Contributed equally.

Correspondence: Anne Dubart-
Kupperschmitt, M.D., Ph.D.,
INSERM UMR S972, Paul Brousse
Hospital, Villejuif, F-94807,
France. Telephone: 00 33 (1) 45
59 51 38; E-Mail: anne.dubart@
inserm.fr

ABSTRACT

Human induced pluripotent stem cells (hiPSCs) hold great promise for cell therapy through their use as vital tools for regenerative and personalized medicine. However, the genomic integrity of hiPSCs still raises some concern and is one of the barriers limiting their use in clinical applications. Numerous articles have reported the occurrence of aneuploidies, copy number variations, or single point muta-tions in hiPSCs, and nonintegrative reprogramming strategies have been developed to minimize the impact of the reprogramming process on the hiPSC genome. Here, we report the characterization of an hiPSC line generated by daily transfections of modified messenger RNAs, displaying several geno-mic abnormalities. Karyotype analysis showed a complex genomic rearrangement, which remained stable during long-term culture. Fluorescent in situ hybridization analyses were performed on the hiPSC line showing that this karyotype is balanced. Interestingly, single-nucleotide polymorphism analysis revealed the presence of a large 1q region of uniparental disomy (UPD), demonstrating for the first time that UPD can occur in a noncompensatory context during nonintegrative reprogram-ming of normal fibroblasts. STEM CELLS TRANSLATIONAL MEDICINE 2015;4:224–229

INTRODUCTION

Aneuploidies, copy number variations (CNVs) [1, 2], and point mutations [3] have been reported as fre-quent genomic aberrations of human induced pluripotent stem cells (hiPSCs), including those gen-erated using nonintegrative reprogramming strate-gies. Some of these mutations are pre-existing in the somatic cell population [4, 5], and others are acquired during the reprogramming process or during early passages [1, 6]. Apart from one article demonstrating that the level of genomic instability is positively cor-related with hiPSC tumorigenic potential [7], the link between genomic integrity and tumorigenesis is poorly studied. Here we report the characterization of a modified messenger RNA (mmRNA)-derived hiPSC line exhibiting a complex but stable and bal-anced chromosomal rearrangement and a large de novo region of uniparental disomy on chromosome 1q. Interestingly, the genomic rearrangements do not impact the iPSC line characteristics in terms of stemness-marker expression and of in vitro sponta-neous differentiation potential, but it impairs the in-duced pluripotent stem cell (iPSC) line ability to generate teratomas in vivo.

MATERIAL AND METHODS

hiPSC Generation and Characterization

The generation, characterization, and culture con-ditions of the mmRNA-derived hiPSC lines have been fully described [8]. Briefly, human foreskin fibroblasts (ATCC, CRL 2097) were transfected daily with a homemade mmRNA cocktail encoding OCT4, SOX2, KLF4, c-MYC, and LIN28 (stoichiome-try 3:1:1:1:1) following a protocol adapted from Warren et al. [9].

Differentiation Potential

The protocols for embryoid bodies and teratoma formation, as well as directed differentiation into specialized cell types, are fully described in the supplemental online data.

Genomic Analyses

Karyotype and fluorescent in situ hybridization (FISH) were performed on the A1 iPSCs cultured on mouse embryonic fibroblast feeder cells (GlobalStem). The A1 iPSCs were cultured on Gel-trex for three passages before genomic DNA extraction for single-nucleotide polymorphism
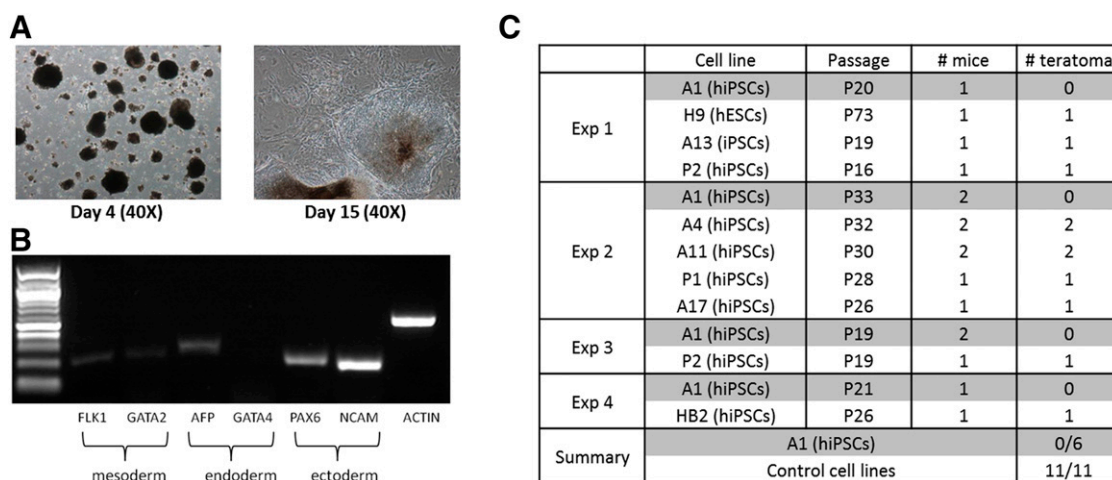
Figure 1. Differentiation potential of the hiPSC line A1. **(A)**: Embryoid body morphology before (day 4) and after (day 15) attachment on a gelatin-coated dish. **(B)**: Expression of germ layer genes *FLK1*, *GATA2*, *AFP*, *GATA4*, *PAX6*, and *NCAM* analyzed by reverse transcription-polymerase chain reaction. **(C)**: Table recapitulating the different attempts of teratoma formation for hiPSC line A1 with control cell lines used. Abbreviations: *AFP*, alpha fetoprotein gene; Exp, experiment; *FLK1*, fetal liver kinase 1/vascular endothelial growth factor receptor 2 gene; *GATA2*, GATA binding protein 2 gene; hiPSCs, human induced pluripotent stem cells; *GATA4*, GATA binding protein 4 gene; *NCAM*, neural cell adhesion molecule gene; *PAX6*, Paired box protein 6 gene.

(SNP) 6.0 and comparative genomic hybridization array analyses. Protocols can be found in the supplemental online data.

RESULTS AND DISCUSSION

hiPSC Generation and Characterization

The clone A1 was picked, expanded, and characterized together with several other hiPSC clones. The morphology of hiPSC line A1 in culture was typical of pluripotent stem cells; small cells with high nucleocytoplasmic ratio (supplemental online Fig. 1A). The expression of the stemness was shown by reverse transcription (RT)-polymerase chain reaction (PCR) (supplemental online Fig. 1C), and the hiPSC line was positive for alkaline phosphatase activity (supplemental online Fig. 1D). Additionally, immunostaining confirmed the presence of the proteins OCT4, NANOG, SSEA4, and TRA-1-60 (supplemental online Fig. 1B), supporting the results obtained on a transcriptional level. Finally, flow cytometry analysis revealed that 90% and 98% of the cells expressed TRA-1-81 and SSEA4, respectively (supplemental online Fig. 1E). Therefore, hiPSC line A1 was indistinguishable from the other hiPSC lines in terms of morphology, stemness phenotyping, and growth rate.

Differentiation Potential

The spontaneous differentiation capacity of the hiPSC line was validated in vitro by generating embryoid bodies (Fig. 1A). RT-PCR confirmed the presence of derivative cells of all three germ layers in these embryoid bodies (Fig. 1B). Subsequently, the pluripotency was analyzed in vivo through generating teratomas after the intramuscularly injection of the cells into immunodeficient mice (Fig. 1C). Surprisingly, in the first experiment, we observed that injected A1 hiPSCs failed to generate teratomas, whereas all the seven control iPSC lines formed teratomas composed of derivatives of the three germ layers (data not shown). We confirmed these results in three independent experiments (experiments 2–4). In summary, none of the six mice injected with A1 hiPSCs developed teratomas, whereas all of the 11 mice injected with control pluripotent stem cell lines developed teratomas.

Because A1 iPSCs did not generate teratomas in vivo, we proceeded to confirm the results obtained from embryoid body test by further in vitro directed differentiation of the cells into specialized cells from the three germ layers. As endoderm-derived cells, we differentiated A1 iPSCs into hepatoblasts expressing AFP (α-fetoprotein) and HNF3β (hepatocyte nuclear factor 3β), two hepatic progenitor specific proteins (Fig. 2A). To investigate the ectoderm differentiation potential, we generated retinal pigmented epithelium (RPE) displaying the typical morphology of RPE cells (flaveolate cells) expressing the specific combination of MITF (microphthalmia-associated transcription factor) and ZO-1 (tight junction's protein) proteins (Fig. 2B). Finally, we differentiated the A1 hiPSCs into mesenchymal cells expressing α-smooth muscle actin, Vimentin, and Calponin (Fig. 2C; supplemental online Fig. 2). These cells were CD105-, CD73-, and CD90-positive and CD31- and CD34-negative, as shown by flow cytometry (supplemental online Fig. 2). Altogether, these experiments confirmed that the hiPSC line A1 is pluripotent in vitro. Regarding in vivo differentiation potential, the absence of teratoma formation in our experiments could be explained by a partially reprogrammed state; however, we do not support this hypothesis because the iPSC line maintained the pluripotent stem cell characteristics and the differentiation capacity in vitro. Moreover, altering the conditions of cell injections may have resulted in the generation of teratomas, such as the addition of adjuvants or using more cells. However, these experiments were not performed for ethical reasons. Therefore, we cannot fully confirm that the iPSC line A1 is unable to form teratomas but rather that its capacity is impaired.

Complex, Balanced, and Stable Chromosomal Rearrangement

In order to assess the chromosomal stability of the hiPSC line, karyotypic analysis was carried out. In contrast to the other hiPSC lines generated in parallel displaying the parental normal karyotype, we found that the A1 hiPSCs exhibited a de novo complex and rare chromosomal rearrangement. The karyotype showed a chromosome 1 with an abnormal short arm, der(1); a derivative
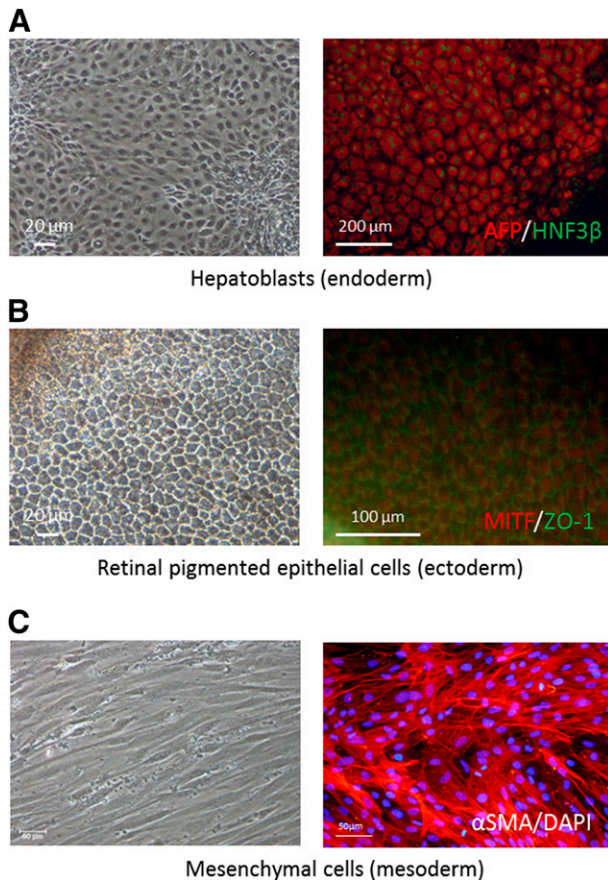
Figure 2. In vitro differentiation of human induced pluripotent stem cell line A1 into specialized cells. **(A)**: Hepatoblasts showing the presence of the proteins AFP/HNF3β by immunostaining. **(B)**: Retinal pigmented epithelial cells showing the presence of the proteins MITF/ZO-1 by immunostaining. **(C)**: Mesenchymal cells showing the presence of αSMA by immunostaining. Abbreviations: DAPI, 4′,6-diamidino-2-phenylindole; HNF3β, hepatocyte nuclear factor 3β/forkhead box protein A2 (FOXA2); MITF, microphtalmia-associated transcription factor; αSMA, α-smooth muscle actin; ZO-1, zona occludens-1/tight junction protein 1 (TJP1).

chromosome 8, der(8); two derivative chromosomes 11, der(11); a derivative chromosome 21, der(21); and the absence of one chromosome 22 (arrows in Fig. 3). FISH analyses were performed to further characterize this rearrangement. The derivative chromosome 1 was exclusively composed of chromosome 1 genomic material (Fig. 3B, 3D) with the insertion of α-sat centromeric DNA sequences near the long-arm extremity (Fig. 3C); short- and long-arm subtelomeric extremities were well localized (Fig. 3E). The two derivative chromosomes 11 resulted from a chromosome 11 break near the centromere. One derivative carried the chromosome 11 short-arm subtelomere and, more likely, a neo-centromere (Fig. 3F–3H), and the other derivative contained chromosome 11 long-arm subtelomere and centromere (Fig. 3I–3K). The derivative chromosomes 8 and 21 were results of a complex reciprocal translocation between a chromosome 8, a chromosome 21, and a chromosome 22 with breakpoints estimated at 8q11.1, 21p11.1, and 22q11.1 regions, respectively. The derivative of chromosome 21 was composed of a chromosome 8 long arm, a chromosome 21 centromeric region, and a chromosome 21 long arm (Fig. 3L–3O). The derivative of chromosome 8 was composed of a chromosome 8 short arm, a chromosome 8 centromeric region, and a chromosome 22 long arm (Fig. 3P–3S).

The resulting chromosomal formula was as follows: 46,XY, der(1),der(8),der(21),rec(11),+rec(11); .ish.der(1)(CEB108/T7+, D1Z5+,wcp1+,D1Z5-,1QTEL10+),der(8)t [8;21;22](q11.1;p11.1; q11.1)(D8S504+,wcp8+;D8Z2+,wcp22+,MS607+),der(21)t [8;21; 22](q11.1;p11.1;q11.1)(VIJyRM2053+,wcp8+;D13Z1/D21Z1+wcp21+, VIJyRM2029+),rec(11)(D11Z1+,wcp11+,D11S1037+),+rec (11)(D11S2071+,wcp11+,D11Z1-).

Interestingly, the karyotype of this cell line at early (passage 16), intermediate (passage 30), and late (passage 54) passages was found to be identical with no occurrence of additional chromosomal events. This showed that the rearrangement acquired during reprogramming or early passages, although complex, was stable throughout long-term propagation. Moreover, we previously demonstrated that A1 iPSCs were able to efficiently differentiate into specialized cells from all three germ layers, confirming that this large genomic rearrangement is not a barrier to differentiation in vitro. In the case of hepatocyte differentiation, this finding has also been shown recently with aneuploid human iPSCs [10]. Our data not only corroborate this finding but also broaden this result for three completely different cell types, using an hiPSC line with a particularly complex karyotype.

hiPSC Line A1 Displayed a Large Region of 1q Uniparental Disomy

Affymetrix SNP 6.0 microarray analysis was performed on both the parental fibroblasts and the hiPSC line A1. Interestingly, compared with the parental fibroblasts and using our criteria ($\geq$100 kb, $\geq$20 markers), no additional CNVs were detected in the hiPSC line A1, indicating that this complex chromosomal rearrangement was balanced around the breakpoints underlined by the karyotype analysis. However, the hiPSC line A1 presented a region with 584 consecutive SNP loci showing a loss of heterozygosity on chromosome 1q when compared with parental fibroblasts, without a loss of genomic material as determined by CNV analysis (Fig. 4). These data indicate the presence of a large de novo uniparental disomy (UPD) of the long arm of chromosome 1 from position 144,988,936 to position 249,143,646 (i.e., 104 Mb including 1,087 genes) (OMIM database). Importantly, no UPD was detected in the seven other iPSC lines derived from the same fibroblasts that were analyzed in parallel (five mmRNA-derived and two retroviral-derived hiPSC lines) [8]. In order to assess the presence of the UPD in the initial population of fibroblasts, three detection attempts were performed in two different samples of the fibroblasts that were used for reprogramming (at passage 6). No UPD was detected based on our SNP genotyping platform, suggesting that these abnormalities may have been generated during the reprogramming process itself or at early passaging stages of the cells. However, if UPD was present in a small percentage of the fibroblasts, it would go undetected because of the limited sensitivity of this technique. To accurately address this question, more resolute techniques such as droplet digital PCR or deep sequencing would be necessary.

Interestingly, UPD has never been reported in hiPSCs until recently [11]. The authors used fibroblasts from patients affected with Miller-Dieker syndrome, with the presence of a ring chromosome 17, and reprogrammed them into hiPSCs using episomal vectors. They showed that multiple hiPSC lines generated do not have the ring chromosome, suggesting the participation of a compensatory UPD mechanism. Our data confirm that UPD can occur, even in a noncompensatory context, during
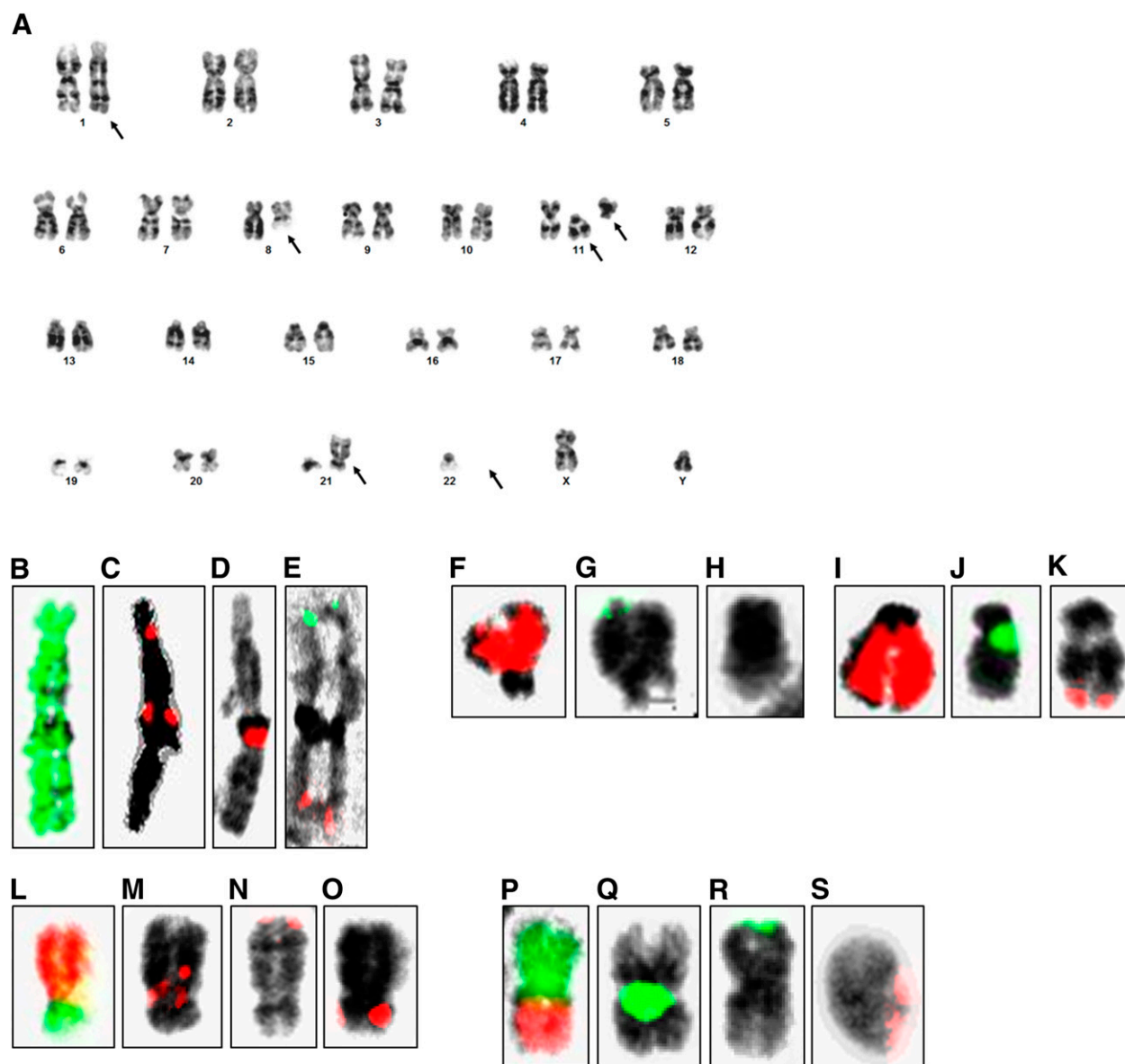
Figure 3. Cytogenetic analyses of the hiPSC line A1: karyotype and fluorescence in situ hybridization (FISH) analyses. **(A)**: Conventional cytogenetic methods: representative standard karyotype (G-bands by trypsin using Giemsa) of A1 cell line at passage 30 showing a male abnormal karyotype with several structural abnormalities (arrows): a derivative chromosome 1 (der[1]), a derivative chromosome 8 (der[8]), two derivative chromosomes 11 (der[11]), a derivative chromosome 21 (der[21]) and the absence of one chromosome 22. **(B–S)**: FISH analysis for derivatives of chromosomes 1 **(B–E)**, 11 (short arm derivative **[F–H]**; long arm derivative **[I–K]**), 8/21 **[L–O]**, and 8/22 **[P–S]** in A1 cell line at passages 19 and 30. **(B)**: Whole painting probes (wpc) 1 (spectrum green). **(C)**: Chromosome enumeration probe (CEP) 1 α-sat (spectrum red). **(D)**: CEP1 satIII (spectrum red). **(E)**: Subtelomere 1pter (spectrum green) and subtelomere 1qter (spectrum red). **(F, I)**: wcp11 (spectrum red). **(G)**: Subtelomere 11pter (spectrum green). **(H, J)**: CEP11 (spectrum green). **(K)**: Subtelomere 11qter (spectrum red). **(L)**: wcp8 (spectrum red)/wcp21 (spectrum green). **(M)**: CEP21 (spectrum red). **(N)**: Subtelomere 8qter (spectrum red). **(O)**: Subtelomere 21qter (spectrum red). **(P)**: wcp8 (spectrum green)/wcp22 (spectrum red). **(Q)**: CEP8 (spectrum green) **R**: Subtelomere 8pter (spectrum green). **(S)**: Subtelomere 22qter (spectrum red).

nonintegrative reprogramming of normal fibroblasts. The functional consequences of UPD are significant; UPD may lead to an imbalance of paternal versus maternal genetic information (which may trigger dysfunction in the case of the presence of imprinted genes in the implicated genome region) or may result in the acquisition of homozygosity for a recessive allele involved in a genetic disorder [12]. Therefore, the presence of UPD should be regarded as an important genomic defect. Because we have shown that UPD can occur during the reprogramming process or early iPSC colony expansion, further studies are required to determine its frequency and the subsequent functional impact on the cells, independent of any karyotype abnormality. These findings also underline the added value of SNP microarray analysis as being the only available approach enabling an accurate detection of regions with consecutive loss of heterozygosity. Regarding the impaired capacity of this iPSC line to form teratoma in vivo (while conserving a large differentiation potential in vitro), we support the hypothesis that there is a direct relationship between this phenotype in vivo and the genotype alterations we describe (especially the UPD because the karyotype
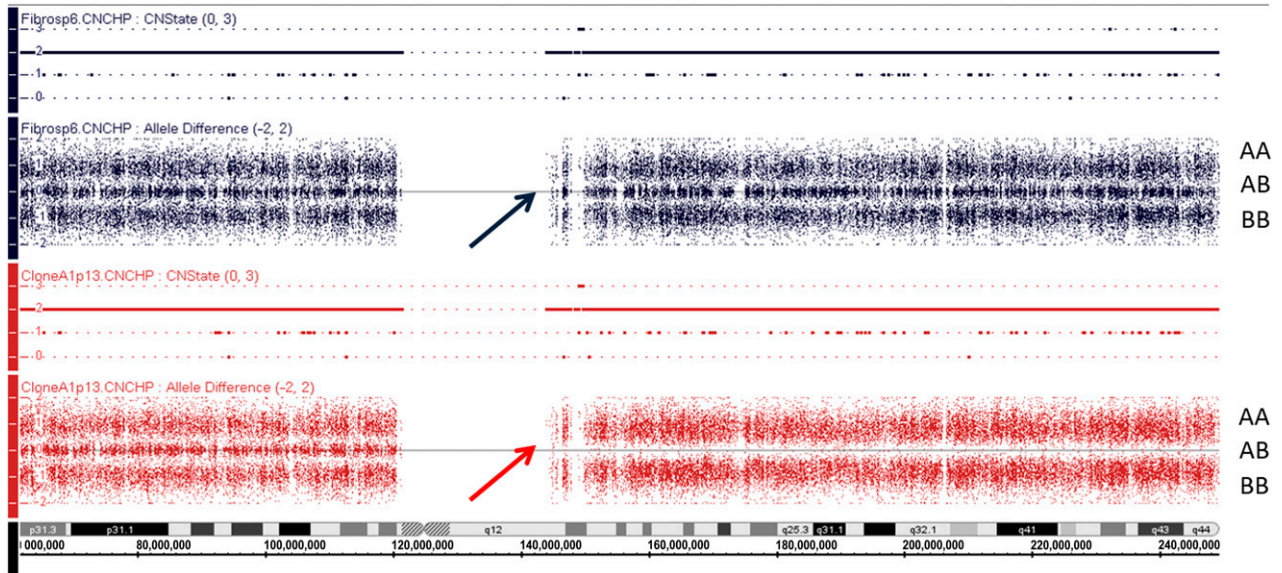
Figure 4. Large de novo uniparental disomy on chromosome 1q of human induced pluripotent stem cell (hiPSC) line A1. Visualization of a large de novo uniparental disomy of chromosome (Chr) 1q in A1 hiPSC line (clone A1, red) when compared with parental fibroblast cell line (FibroSp6, black). Allele difference section revealed a loss of heterozygosity (red arrow) on Chr 1q in hiPSC line A1 compared with Chr 1q parental fibroblast cell line (black arrow) and Chr 1p of the same line. Copy number analysis (horizontal lines) did not show any copy number variation of Chr 1q in either parental fibroblast (black lines) or hiPSC line A1 (red lines).

is balanced), which may be due to a defect in cell migration or implantation pathways. However, exploring this relationship was beyond the scope of this work.

CONCLUSION

This work demonstrates that an hiPSC line, generated with a non-integrative reprogramming strategy, may harbor an abnormal, complex, and stable karyotype, which in turn does not impact the pluripotent stem cell in vitro characteristics and differentiation potential. The teratoma formation capacity is impaired in this cell line, but further investigations are required to establish the relationship between this feature and its genetic characteristics. This study also demonstrates that UPD can occur during the reprogramming process or at early passages, and further studies looking for UPDs are required to determine the frequency of occurrence in iPSCs with normal karyotypes and the subsequent functional importance. UPD detection could only be performed through SNP analysis. This highlights the importance of combining karyotyping with complementary genomic analyses and further enforcing the use of SNP analysis as a routine screening method for quality control of hiPSC lines suitable for clinical applications.

AUTHOR CONTRIBUTIONS

C.S.: conception and design, collection and assembly of data, data analysis and interpretation, manuscript writing; J.M.: collection and assembly of data, data analysis and interpretation; L.T.: collection and assembly of data, data analysis and interpretation, manuscript writing; E.L., D.P., and N.D.: collection and assembly of data; Z.H.: data analysis and interpretation, manuscript writing; G.T. and J.M.: conception and design, data analysis and interpretation, manuscript writing; A.D.-K.: conception and design, data analysis and interpretation, manuscript writing, final approval of the manuscript.

DISCLOSURE OF POTENTIAL CONFLICTS OF INTEREST

The authors indicated no potential conflicts of interest.

REFERENCES

1 Hussein SM, Batada NN, Vuoristo S et al. Copy number variation and selection during reprogramming to pluripotency. Nature 2011; 471:58–62.

2 Laurent LC, Ulitsky I, Slavin I et al. Dynamic changes in the copy number of pluripotency and cell proliferation genes in human ESCs and iPSCs during reprogramming and time in culture. Cell Stem Cell 2011;8:106–118.

3 Gore A, Li Z, Fung HL et al. Somatic coding mutations in human induced pluripotent stem cells. Nature 2011;471:63–67.

4 Abyzov A, Mariani J, Palejev D et al. Somatic copy number mosaicism in human skin revealed by induced pluripotent stem cells. Nature 2012;492:438–442.

5 Young MA, Larson DE, Sun CW et al. Background mutations in parental cells account for most of the genetic heterogeneity of induced pluripotent stem cells. Cell Stem Cell 2012;10:570–582.

6   Ji J, Ng SH, Sharma V et al. Elevated coding mutation rate during the reprogramming of human somatic cells into induced pluripotent stem cells. STEM CELLS 2012;30:435–440.

7   Liang Y, Zhang H, Feng QS et al. The propensity for tumorigenesis in human induced pluripotent stem cells is related with genomic instability. Chin J Cancer 2013;32:205–212.

8   Steichen C, Luce E, Maluenda J et al. Messenger RNA- versus retrovirus-based induced pluripotent stem cell reprogramming strategies: Analysis of genomic integrity. STEM CELLS TRANSLATIONAL MEDICINE 2014;3:686–691.

9   Warren L, Manos PD, Ahfeldt T et al. Highly efficient reprogramming to pluripotency and directed differentiation of human cells with synthetic modified mRNA. Cell Stem Cell 2010;7:618–630.

10   Noto FK, Determan MR, Cai J et al. Aneuploidy is permissive for hepatocyte-like cell differentiation from human induced pluripotent stem cells. BMC Res Notes 2014;7: 437.

11   Bershteyn M, Hayashi Y, Desachy G et al. Cell-autonomous correction of ring chromosomes in human induced pluripotent stem cells. Nature 2014;507:99–103.

12   Robinson WP. Mechanisms leading to uniparental disomy and their clinical consequences. BioEssays 2000;22:452–459.

See www.StemCellsTM.com for supporting information available online.

Subspecialty Collections   This article, along with others on similar topics, appears in the following collection(s):
Pluripotent Stem Cells
http://stemcellstm.alphamedpress.org//cgi/collection/induced-pluripotent-stem-cells **Pluripotent Stem Cells**
http://stemcellstm.alphamedpress.org//cgi/collection/embryonic-stem-cells-induced-pluripotent-stem-cells

An Atypical Human Induced Pluripotent Stem Cell Line With a Complex, Stable, and Balanced Genomic Rearrangement Including a Large De Novo 1q Uniparental Disomy

Clara Steichen, Jérôme Maluenda, Lucie Tosca, Eléanor Luce, Dominique Pineau, Noushin Dianat, Zara Hannoun, Gérard Tachdjian, Judith Melki and Anne Dubart-Kupperschmitt

The online version of this article, along with updated information and services, is located on the World Wide Web at:
http://stemcellstm.alphamedpress.org/content/4/3/224